scientific reports

Check for updates

OPEN

FOXF1 inhibits invasion and metastasis of lung adenocarcinoma cells and enhances anti-tumor immunity via MFAP4/FAK signal axis

Zhenyu Wang[1], MengXia Xie[1], Zhongyue Jia[1], Ziwei Tao[1], Ping Zhao[2] & Muying Ying[1]✉

Based on the joint analysis of multi-omic data and the biological experiments, we demonstrate that FOXF1 inhibits invasion and metastasis of lung adenocarcinoma cells and enhances anti-tumor immunity via regulating MFAP4/FAK signal axis in this study. The levels of FOXF1 and MFAP4 are significantly down-regulated in LUAD, and the increased levels of two genes can improve the clinical prognosis of LUAD patients. Fluorescein reporter gene determination, chromatin immunoprecipitation and gene co-expression analysis indicate that MFAP4 level is positively regulated by transcription factor FOXF1. The function enrichment analysis shows that the levels of FOXF1 and MFAP4 are closely associated with an enrichment of tumor metastasis signatures. FOXF1 can inhibit the migration and invasion of LAUD cells by transcriptionally activating MFAP4 expression. And the overexpression of FOXF1/MFAP4 can reduce focal adhesion kinase (FAK) phosphorylation, while their knockdown result in the opposite effects. The increased levels of FOXF1/MFAP4 enhance the antitumor immunity by increasing the infiltration of dendritic cells and CD4+ T cells, and the interactions between LUAD cells and immune cells, and activating multiple anti-tumor immunity-related pathways. In conclusion, our study reveals the potential function of FOXF1/MFAP4/FAK signal axis in inhibiting metastasis of LUAD cells and modulating anti-tumor immunity of LUAD patients.

Keywords Lung adenocarcinoma, Single-cells RNA sequencing, FOXF1, MFAP4, Focal adhesion kinase, Tumor-infiltrating lymphocytes

Abbreviations

MFAP4	Microfibril associated protein 4
FOXF1	Forkhead box F1
FAK	Focal adhesion kinase
NSCLC	Non-small cell lung cancer
LUAD	Lung adenocarcinoma

Lung cancer is the leading cause of cancer death worldwide and the third most common cancer following breast and prostate[1]. Non-small cell lung cancer (NSCLC) accounts for about 85% of lung cancer, 60% of which is lung adenocarcinoma (LUAD), being the most common histological type of lung cancer[2]. There is a deficiency in optimal predictive biomarkers that can accurately forecast LUAD patient prognoses and guide the selection of targeted treatments. Given the high incidence and mortality, it is essential and urgent to search for novel biomarkers for diagnosis and targeted therapy to improve the survival outcomes of LUAD patients.

Forkhead box F1 (FOXF1) belongs to the forkhead family of transcription factors which is characterized by a distinct forkhead domain, and may play a role in the regulation of pulmonary genes and embryonic development.

[1]Department of Molecular Biology and Biochemistry, School of Basic Medical Sciences, Jiangxi Medical College, Nanchang University, Nanchang 330031, China. [2]The First Affiliated Hospital Zhejiang University School of Medicine, Zhejiang 310000, China. ✉email: yingmuying@ncu.edu.cn

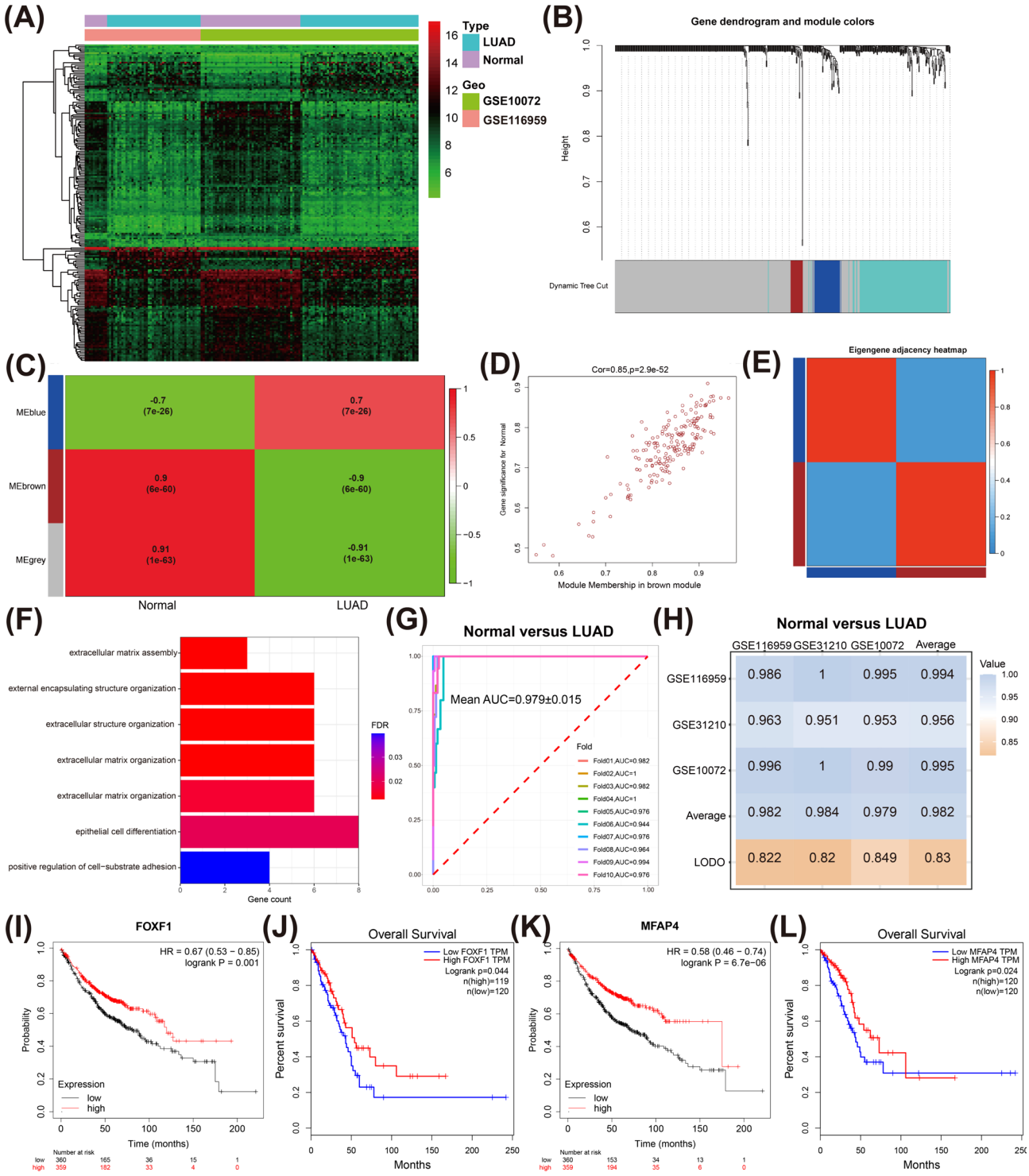

Previous study indicates a crucial role of FOXF1 in endothelial progenitors and connected vascular sprouting as it may be relevant for tissue neovascularization[3]. The increased level of FOXF1 inhibited NSCLC growth by activating tumor suppressor p21 and G1 cell-cycle arrest[4]. FOXF1 can induce epithelial mesenchymal transformation in colorectal cancer and affect its metastasis through transcriptional activation of SNAI1[5]. T Highly expressed FOXF1 can inhibit the expression of cyclin by activating tumor suppressor p21, which leads to cell cycle arrest in GAP1 phase and inhibits the proliferation of LUAD cells[6]. Depending on tissue and histological type of cancer, FoxF1 has been shown to be either an oncogene or a tumor suppressor, and the mechanism of FOXF1 affecting LUAD tumor metastasis is still not clear[7].

Microfibril associated protein 4 (MFAP4) is an extracellular matrix protein which is involved in cell adhesion or intercellular interactions, and has binding specificities for both collagen and carbohydrate. MFAP4 belongs to the superfamily of fibrinogen-related protein, which is also an important regulatory factor in regulating airway

◂**Fig. 1.** Key genes related to the progression of LUAD are discovered by performing WGCNA and random forest algorithm. (**a**) Heatmap showing the common top 100 differentially expressed genes (DEGs) of GSE10072 and GSE116959 datasets between normal and LUAD samples. (**b**) Clustering dendrogram of all DEGs based on the measurement of dissimilarity. Color bar showing results obtained from automated single block analysis. (**c**) Module-trait association: each row corresponds to a module and each column corresponds to a trait. (**d**) A scatter plot for Gene Significance (GS) versus Module Membership (MM) in brown module. (**e**) Eigengene adjacency heatmap of blue and brown module. (**f**) Histogram showing genes in brown modules enriched in signal pathways associated with cell adhesion and extracellular matrix. (**g**) ROC curves of tenfold cross-validation of all cell adhesion and extracellular matrix-related genes using Random Forest algorithm (Normal vs LUAD, data from TCGA database). (**h**) The results of mutual cross-validation of the three datasets (GSE10072, GSE116959, GSE31210) by using Random Forest algorithm. Values on the diagonal are the results of cross-validation for each dataset. The off-diagonal values refer to the AUC values obtained by cross-cohort validation, which trains the classifier on the study of the corresponding column and applies it to the dataset of the corresponding row. The LODO value refers to the performance obtained by training a classifier with all datasets except the dataset corresponding column. (**i**) The association between the expression of PECAM1, A2M, TCF21, MFAP4, FOXF1 and LUAD patients' Overall Survival in GEPIA database. The "WGCNA" package (version 1.7.2, http://horvath.genetics.ucla.edu/html/CoexpressionNetwork/Rpackages/WGCNA/) in R was used to build a co-expression network. The "Pheatmap" (version 1.0.12, https://github.com/raivokolde/pheatmap) and "ggplot2" (version 3.5.0, https://github.com/tidyverse/ggplot2) packages in R were used to plot the heatmap. Survival plots were generated from the GEPIA database (http://gepia.cancer-pku.cn/).

smooth muscle cell regeneration, inducing the proliferation and migration of vascular smooth muscle cells, chemotaxis of monocytes, and neointimal hyperplasia after vascular injury[8]. High expression of MFAP4 predict primary Platinum-based chemoresistance and are associated with adverse prognosis in patients with serous ovarian cancer[9]. As a target gene of microRNA-147b, MFAP4 can affect the migration and invasion of LUAD cells[10]. As an excessive extracellular matrix protein that interacts with elastin and collagen, MFAP4 deficiency alleviates renal fibrosis through inhibition of NF-κB and TGF-β/Smad signaling pathways[11].

Previous studies have indicated that both FOXF1 and MFAP4 play an essential role in the occurrence and development of LUAD, while we do not yet know whether there are regulatory relationships between these two genes in the molecular mechanism of the development of lung cancer. In the present study, we elucidate the transcription regulation mechanism of FOXF1 on MFAP4 and find FOXF1 can inhibit the migration and invasion of LUAD cells by positively regulating the expression of MFAP4. And the increased levels of FOXF1/MFAP4 can reduce the phosphorylation level of focal adhesion kinase (FAK), a key molecule in FAK signal pathway, indicating a role of FAK signal pathway in the inhibition of LUAD metastasis by FOXF1/MFAP4. And also, our results indicate that the increased levels of FOXF1/MFAP4 can enhance the anti-tumor immunity of LUAD patients, which may be closely related to their promotion in the function of CD4+ T cells and dendritic cells (DCs). In conclusion, our study demonstrates the functional mechanism of FOXF1-MFAP4-FAK signal axis in LUAD metastasis and FOXF1/MFAP4-mediated anti-tumor immunity.

Results

Analysis of differentially expressed genes and hub genes identification

Through joint differential expression analysis of the data in GSE116959 and GSE10072, 574 Differentially expressed genes (DEGs) between LUAD and lung normal samples are identified, including 190 up-regulated genes and 388 down-regulated genes (Table S1). The heatmap of the Top 200 DEGs screened according to the absolute value of Fold Change (FC) are shown in Fig. 1a. With "WGCNA" package, we constructed a DEGs-co-expression network to classify DEGs with highly relevant expression patterns into modules by average linkage clustering, and the power of $\beta = 30$ (scale free $R^2 = 0.90$) and a cut-off modules size = 30 were set as the soft threshold to ensure a scalefree network. After merging similar modules with the MED > 0.25 as threshold, three modules were generated accordingly (Fig. 1b). As shown in Fig. 1c, analyzing the correlation between gene expression and normal or cancerous characteristics indicates that the brown module is the module with the strongest negative correlation with LUAD ($R = -0.9$, $p = 6e{-}60$). Therefore, we defined brown module as the hub module. The intramodular analysis for gene significance (GS) and module membership (MM) further exhibit a very significantly negative correlation in the brown module with LUAD ($p = 2.9e{-}52$, $R = 0.85$, Fig. 1d). Figure 1e shows the correlation between blue and brown modules. Figure 1f exhibit the functional enrichment analysis results associated with distant metastasis of LUAD by performing GO analysis of 136 genes from brown module. By analyzing the above enriched functional pathways related to LUAD metastasis and progress, we obtained 18 DEGs related to LUAD distant metastasis and defined it as a LUAD-progress-related signature. Then we used the signature to establish a random forest model, and performed tenfold-cross-validation[12] using Bulk RNA-Seq data from TCGA database and plotted Receiver Operating Characteristic (ROC) curves (Fig. 1g), which indicates that the above DEGs has great performance in distinguishing normal and LUAD samples (Mean AUC = 0.979 ± 0.015). In order to further ensure the reliability of the results, we conducted multi-sample cross-validation in the GSE116959, GSE10072 and GSE31210 datasets, and the results show that the above LUAD-related signature still has strong reliability in distinguishing normal and tumor samples (Fig. 1h). The survival prognosis analysis of all genes in the metastasis-related signature indicates that PECAM1, A2M, TCF21, MFAP4 and FOXF1 are the most relevant to survival prognosis, and the high expression of both improve the survival status of LUAD patients (Fig. 1i). Figure S1 shows the association between other genes in LUAD-related signature and the overall survival of LUAD.

The above analysis results suggest that PECAM1, A2M, TCF21, MFAP4 and FOXF1 may play an important role in inhibiting the progress of LUAD. And we define these genes as hub genes.

scRNA-Seq profiling reveals the important function of FOXF1 and MFAP4 in LUAD cells' metastasis

As the only transcription factor in hub genes, FOXF1 may play an important regulatory function in the progression of LUAD. To further explore the function of FOXF1 in LUAD, we analyzed the single-cells RNA sequencing (scRNA-Seq) data of LUAD from GSE131907 dataset. Figure 2a and b display the tSNE plot of all cells that are from respectively normal lung tissues, primary LUAD tissues and LUAD tissues at metastatic sites, which are clustered into 21 different cell clusters. The bubble plot shows the expression of the characteristic maker genes of immune cells, epithelial cells and stromal cells in different cell clusters (Fig. 2c). According to the expression of the maker genes, all cells are initially divided into immune cells, epithelial cells and stromal cells (Fig. 2d). Next, we calculated the CNV of all epithelial cells using the "inferCNV" package. By calculating CNV levels (Fig. 2e), epithelial cells with abnormally high CNV levels (Kmeans3, 4, 5, 6, 7 classes) are identified as malignant epithelial cells (LUAD cells) for subsequent analysis (Fig. 2f). Figure 2g and h display the tSNE plot of all LUAD cells, which are clustered into 8 different cell subpopulations. Figure 2i demonstrates that FOXF1 and MFAP4 are mainly concentrated in LUAD cells from the primary sites (Cluster 6), and the expression levels of the both genes are significantly reduced in the metastatic sites, suggesting a synergistic role of the both genes in the progression of LUAD. According to the functional enrichment results of DEGs from different cell subpopulations, LUAD cells are further divided into 5 different functional clusters, among which the cell populations with the increased levels of FOXF1 and MFAP4 are mainly enriched in intercellular adhesion related functions (Fig. 2j). Pseudotime analysis of all LUAD cells suggest that the group of cell cluster with the increased expression of FOXF1 and MFAP4, namely cluster6, is mainly in the early stage of development, while the LUAD cells in the metastatic site are almost all in the late stage of development (Fig. 2k,l) . The above results imply that the high expression of MFAP4 and FOXF1 may inhibit the distant metastasis of LUAD cells by affecting the adhesion function of LUAD cells.

MFAP4 is identified as the target gene of FOXF1 and its expression is positively regulated by FOXF1

The analysis of the data from the public datasets (TCGA, GSE10072, GSE116959) indicate that both FOXF1 and MFAP4 are significantly down-regulated in LUAD compared with normal lung tissues (Fig. 3a,b). In order to validate the reliability of the results from public datasets, we detected the expression level of FOXF1 and MFAP4 in 3 pairs of LUAD clinical tissues by Western blot and qRT-PCR. Consistently, FOXF1 and MFAP4 are significantly down-regulated in LUAD tissues at both transcriptional and translation levels (Fig. 3c,d). FOXF1 and MFAP4 are clustered into the same module in WGCNA analysis and enriched to the same pathways. In order to explore whether there is a possible regulatory relationship between the two genes, we firstly carried out co-expression analysis, which indicate a significant positive correlation between FOXF1 and MFAP4 expression in multiple datasets (Fig. 3e). qRT-PCR experiment based on the 7 clinical samples of LUAD further validate our date analysis from public datasets (Fig. 3f).

To explore whether FOXF1 regulates the expression of MFAP4, we used LUAD cell lines (A549 cell lines and SPC-A1 cell lines) constructing LUAD cell models of overexpression and knockdown of FOXF1. LUAD cell models of overexpression and knockdown of FOXF1 indicate that the increased expression of FOXF1 promote the expression of MFAP4, while the knockdown of FOXF1 demonstrates inhibitory effects (Fig. 3g–j). Through AnimalTFDB database[13], we predicted the potential binding sites of FOXF1 for MFAP4 (Fig. 3k). The results of double luciferase reporter gene experiment indicate that the overexpression of FOXF1 could significantly increase luciferase activity of MFAP4 promoter (Fig. 3l). Moreover, the qRT-PCR of ChIP assays for FLAG-FOXF1 in A549 and SPC-A1 cells also show that FOXF1 can bind to MFAP4 promoter (Fig. 3m and Fig. S2). These results indicate that FOXF1 can positively regulate the expression of MFAP4 in LUAD.

FOXF1 inhibits the migration and invasion of LUAD cells by transcriptionally activating the expression of MFAP4

In order to explore the specific functions of FOXF1 and MFAP4 in the process of LUAD cells metastasis, we performed cell scratch and Transwell experiments to detect the migration and invasion ability of LUAD cell lines overexpressing or knocking down FOXF1 (Fig. 4a,b). Cell scratch experiments display that the high expression of FOXF1 significantly inhibit the migration of LUAD cells, while its low expression can enhance the migration (Fig. 4c–f). Similarly, Transwell experiments indicate that increasing the expression of FOXF1 could inhibit the invasive ability of LUAD cells, while reducing its expression promote the migration of LUAD cells (Fig. 4g,h).

To demonstrate whether MFAP4 is the target gene of FOXF1 affecting the metastasis of LUAD cells, we carried out rescue experiment on A549 and SPC-A1 cell lines by using small interfering (siRNA) of MFAP4 to target its mRNA degradation in LUAD cell lines (A549 and SPC-A1), while overexpressing FOXF1, and overexpressing MFAP4 in FOXF1 knockdown LUAD cell lines (A549 and SPC-A1), respectively (Fig. 5a–d). Cell scratch and transwell experiments indicate that there is a synergistic function between FOXF1 and MFAP4 in inhibiting the ability of A549 and SPC-A1 cells' migration and invasive (Fig. 5e–l). These results suggest that MFAP4 is the functional target gene of FOXF1 in inhibiting the migration and invasion of LUAD cells.

The overexpression of FOXF1/MFAP4 inhibits the activation of FAK signal pathway

Consisting with our results of scRNA-Seq data analysis, the high expression of FOXF1/MFAP4 is found to be co-enriched in FAK signal pathway. And FOXF1/MFAP4 may affect the metastasis of LUAD cells through affecting

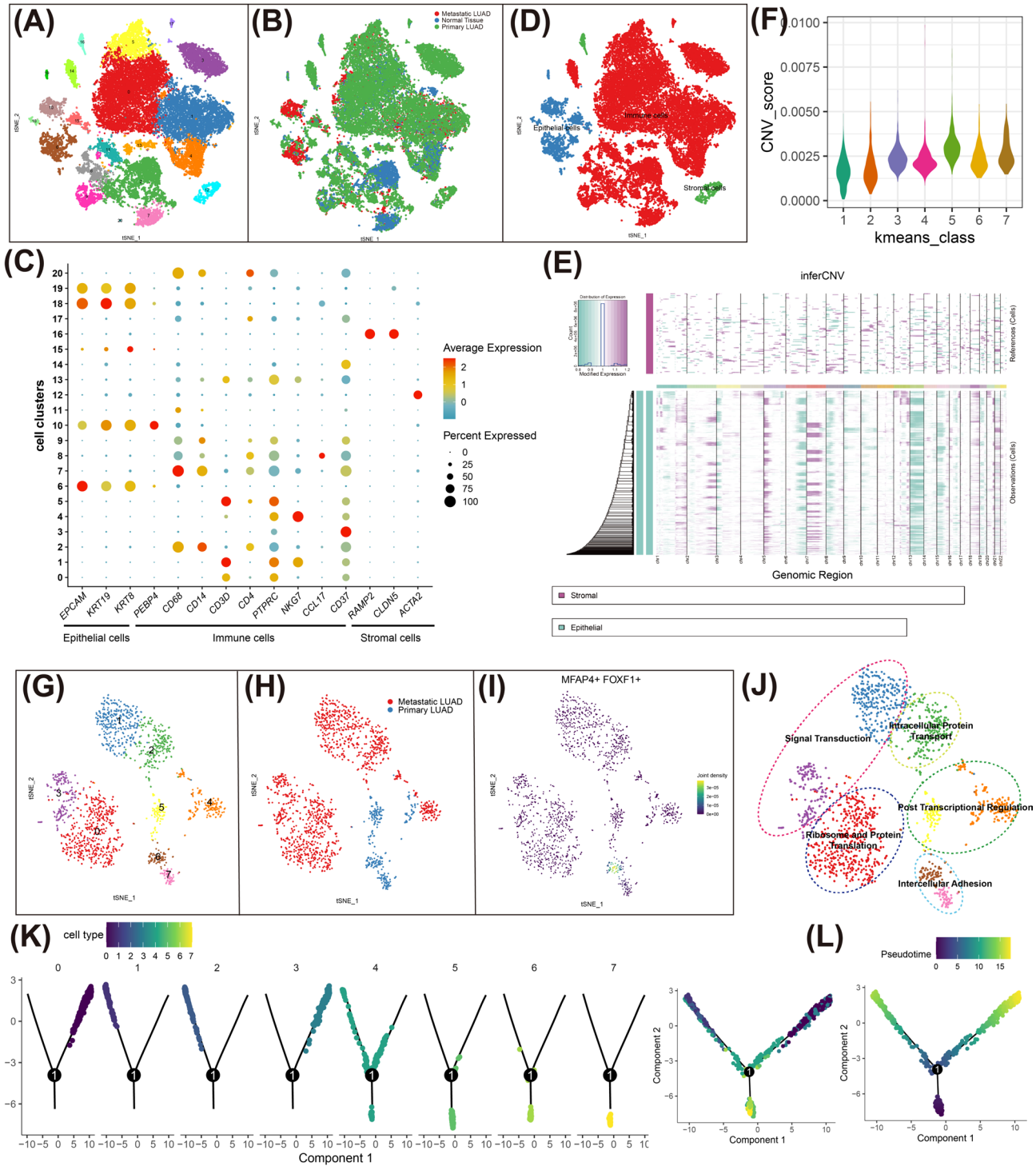

Fig. 2. Single-cell RNA Sequencing (scRNA-Seq) data reveals the vital functions of FOXF1 and MFAP4 in cell adhesion and the metastasis of LUAD cells. (**a**) Using tSNE algorithm to divide all cells into 20 clusters. (**b**) The tSNE plot shows the sources of all cells. (**c**) The bubble plot shows the expression of marker genes used for cell annotation. (**d**) All cells are preliminarily divided into immune cells, epithelial cells and stromal cells. (**e**) Copy number variation (CNV) in epithelial cells and the stromal cells in normal lung tissues are used as reference cells. (**f**) Kmeans algorithm clustering all epithelial cells into 7 clusters according to CNV level. (**g**,**h**) Using tSNE algorithm to reduce the dimensionality of epithelial cells with high CNV level (LUAD tumor cells, Kmeans 3,4,5,6,7) into 7 cell clusters. (**i**) The expression level of FOXF1 and MFAP4 in LUAD tumor cells from different sources. (**j**) Functional enrichment analysis divides LUAD tumor cells into different functional modules. (**k**,**l**) Pseudotime analysis of 7 cell clusters calculated by tSNE algorithm. The tSNE plot was generated from "Seurat" package (version 4.4.0, https://github.com/satijalab/seurat) in R. The "ggplot2" (version 3.5.0, https://github.com/tidyverse/ggplot2) package in R was used to plot the heatmap and the bubble plot.

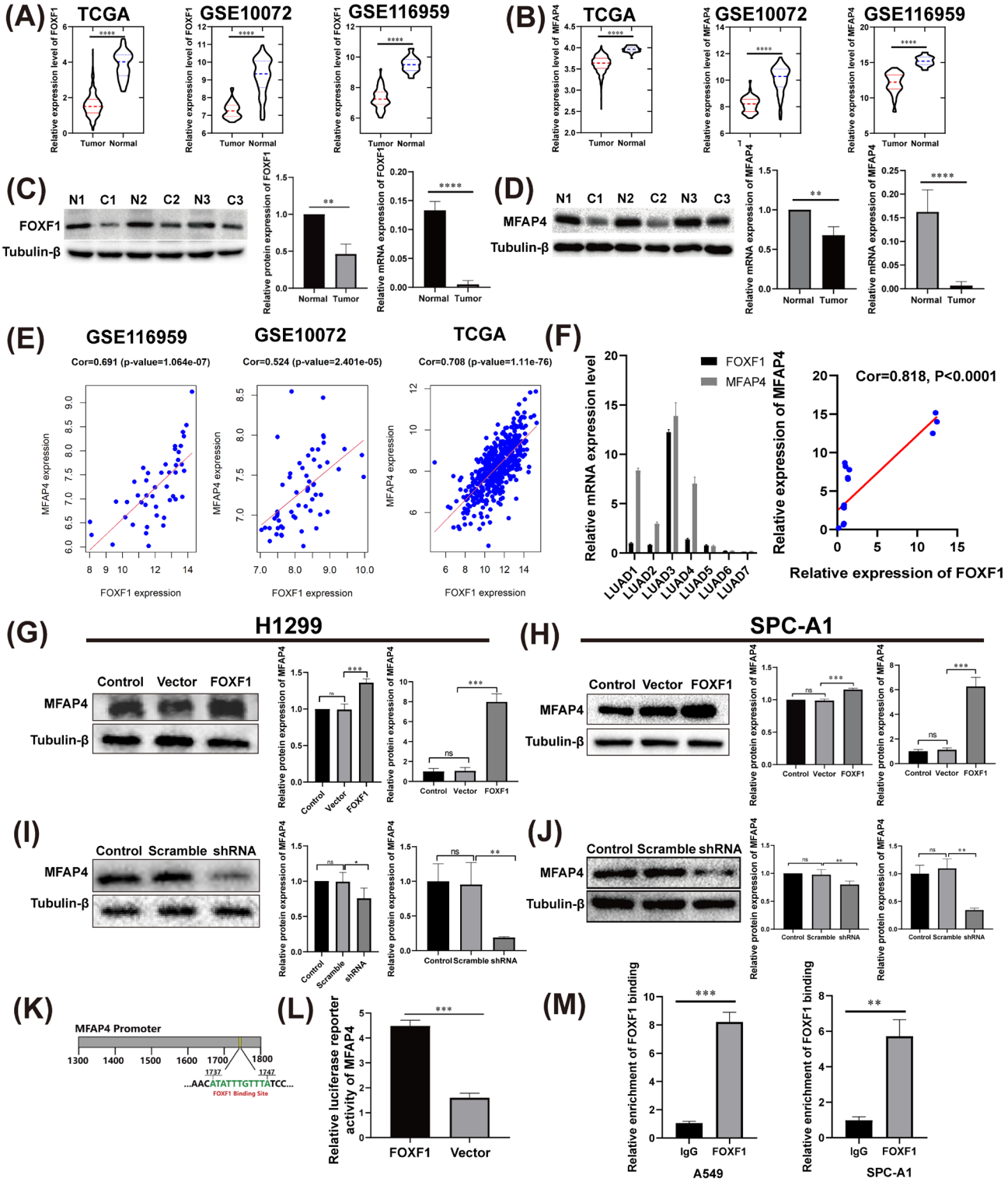

Fig. 3. MFAP4 is a target gene of FOXF1 in LUAD. (**a**,**b**) The mRNA level of FOXF1 and MFAP4 in 3 public datasets (TCGA, GSE10072, GSE116959). (**c**,**d**) The results of Western Blot and qRT-PCR used to analyze the protein and mRNA levels of FOXF1 and MFAP4 in 3 pairs of LUAD clinical samples. (**e**) Co-expression analysis of FOXF1 and MFAP4 by using 3 public datasets (GSE116959, GSE10072, TCGA). (**f**) The expression levels of FOXF1 and MFAP4 in 7 LUAD clinical samples and performing co-expression analysis. (**g**–**j**) Using Western Blot or qRT-PCR to detect the expression of MFAP4 with the overexpression or knockdown of FOXF1 in A549 and SPC-A1 cell lines. (**k**) HumanTFDB predicts the potential binding site of FOXF1 on the promoter of MFAP4. (**l**) Performing double luciferase reporter gene experiment to explore the effect of FOXF1 on the transcriptional activity of MFAP4 promoter in 293 T cells. (**m**) Chromatin Immunoprecipitation (Chip) are performed in A549 and SPC-A1 cells, and qRT-PCR is performed with primers against the indicated area in MFAP4 promoter.

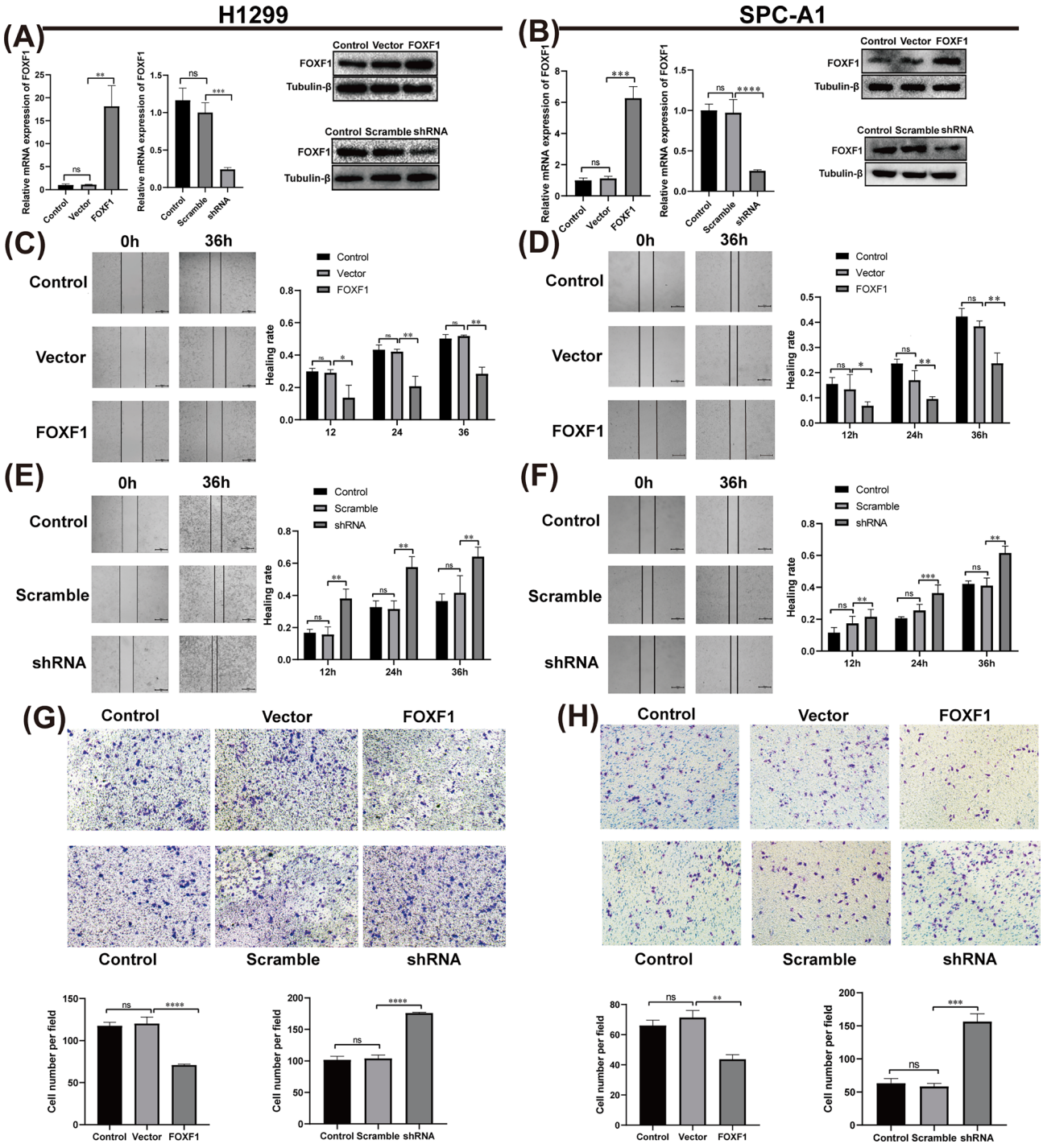

Fig. 4. The high expression of FOXF1 can significantly inhibit the malignant degree of LUAD cells. (**a**,**b**) The cell models of knockdown and overexpression of FOXF1 constructed in A549 and SPC-A1 cells. (**c**,**d**) Cell scratch experiment detecting the effect of overexpression of FOXF1 on the migration ability of A549 and SPC-A1 cells. (**e**,**f**) Cell scratch experiment detecting the effect of knockdown of FOXF1 on the migration ability of A549 and SPC-A1 cells. (**g**,**h**) Transwell experiment detecting the effect of overexpression or knockdown of FOXF1 on the invasion ability of A549 and SPC-A1 cells.

the adhesion ability between LUAD cells (Fig. 6a). Meanwhile, GSEA and ssGSEA also demonstrate that the high expression of FOXF1/MFAP4 is positively correlated with FAK signal pathway (Fig. 6b,c), which may imply the crucial roles of FAK signal pathway in FOXF1/MFAP4 inhibiting the migration and invasion of LUAD. In order to elucidate the specific association between the FAK signal pathway and FOXF1/MFAP4, we detected the expression levels of FAK/phosphorylated FAK (Tyr397) as the expression of FOXF1 and MFAP4 changed. The results

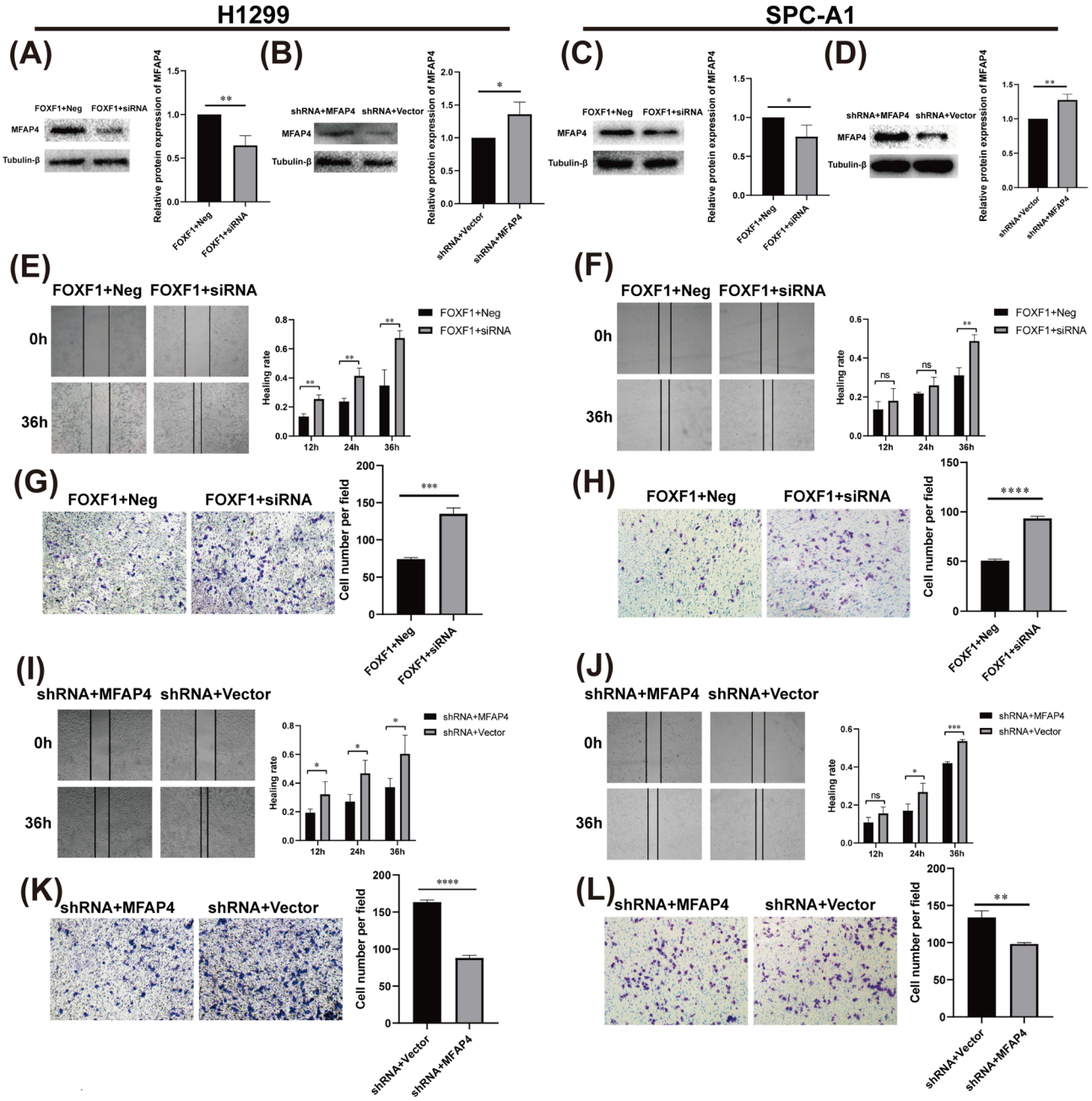

Fig. 5. FOXF1 can inhibit the malignant behaviors of LUAD cells by positively regulating MFAP4 expression. (**a–d**) Relative expression of MFAP4 in A549 and SPC-A1 cells under different transfection conditions. (**e–h**) Knocking down the expression of MFAP4 in LUAD cells (A549 and SPC-A1) overexpressing FOXF1, and detecting the change of migration ability and invasion ability by cell scratch experiment and Transwell experiment. (**i–l**) Overexpressing the expression of MFAP4 in LUAD cells (A549 and SPC-A1) knocking down FOXF1, and detecting the change of migration ability and invasion ability by cell scratch experiment and Transwell experiment.

reveal that the overexpression of FOXF1/MFAP4 reduce the level of FAK phosphorylation, while the increased levels of FAK phosphorylation is observed when the expression level of FOXF1/MFAP4 is decreased (Fig. 6d).

The overexpression of FOXF1/MFAP4 promotes antitumor immunity and enhances intercellular communication

Data analysis of TIMER database indicates that the expression of both FOXF1 and MFAP4 is positively correlated with the infiltration of CD4+ T cells and DCs in LUAD (Fig. 7a–c). The analysis of the association between the expression of key marker genes on CD4+ T cells and DCs with FOXF1 and MFAP4 indicates that the result is consistent with the infiltration of CD4+ T cells and DCs (Fig. 7d), which is validated by qRT-PCR results (Fig. S3). In order to further verify the reliability of the TIMER database analysis, we performed a more

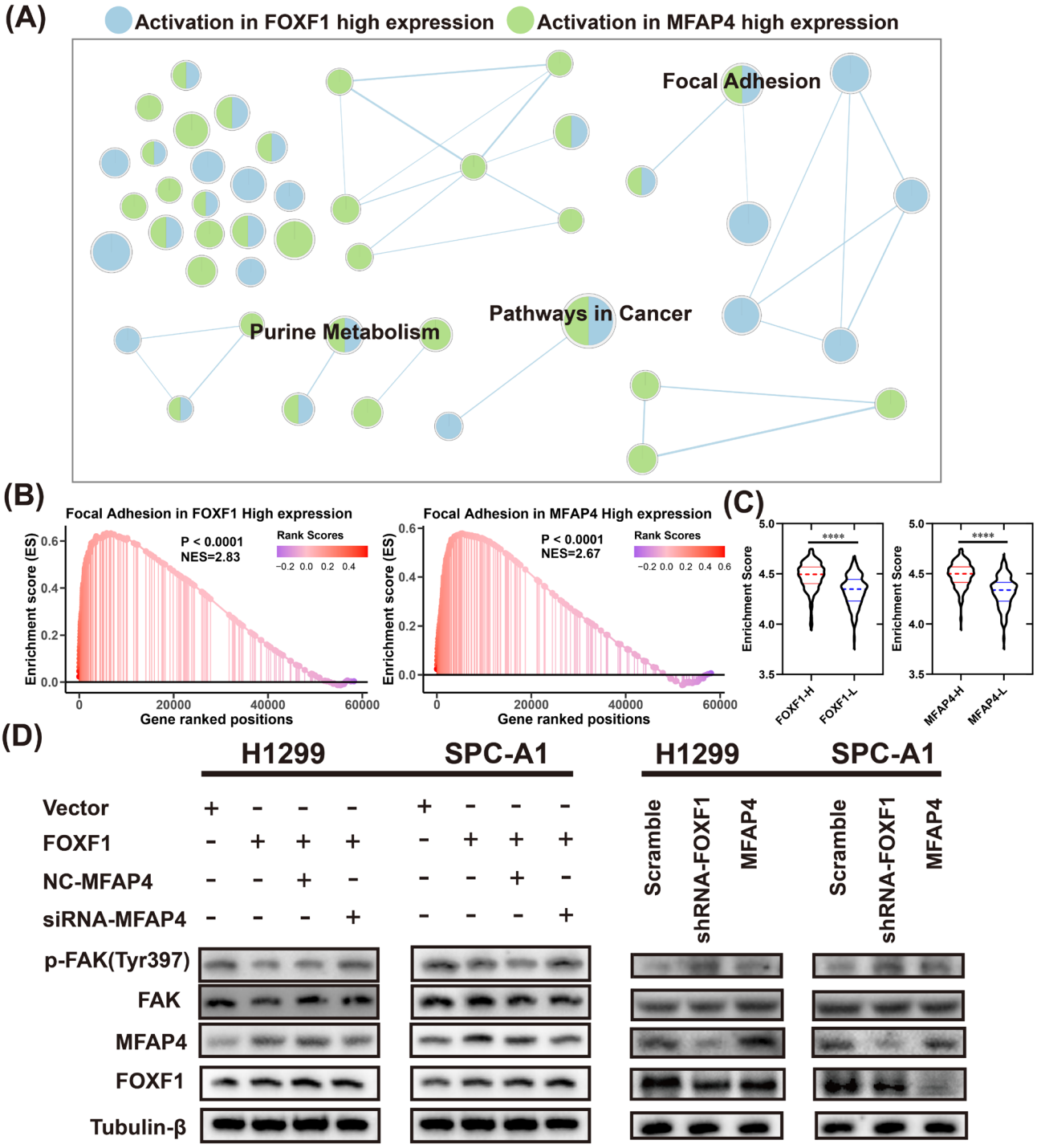

Fig. 6. FOXF1 can affect the activation of FAK signal pathway by regulating the expression of MFAP4. (**a**) The network diagram shows the signal pathways positively related to the high expression of FOXF1 and MFAP4. Green indicates that the activation of signaling pathways is significantly correlated with the expression of FOXF1, and the blue indicates that the activation of signaling pathways is significantly correlated with the expression of MFAP4. The network diagram displays the three signal pathways that are most relevant to both FOXF1 and MFAP4 (Pathways in Cancer, Focal Adhesion, Purine Metabolism). (**b**) GSEA shows that the high expression of FOXF1 and MFAP4 is significantly associated with Focal Adhesion signal pathway. (**c**) ssGSEA indicates that both high expression of FOXF1 and MFAP4 is significantly associated with Focal Adhesion signal pathway. (**d**) Protein expression of FAK and p-FAK (Tyr397) with FOXF1 and MFAP4 expression are detected by Western Blot. The network diagram was generated from "Cytoscape" software (version 3.10.2, https://cytoscape.org/) and the GSEA plots were generated from the "ggplot2" (version 3.5.0, https://github.com/tidyverse/ggplot2) package in R.

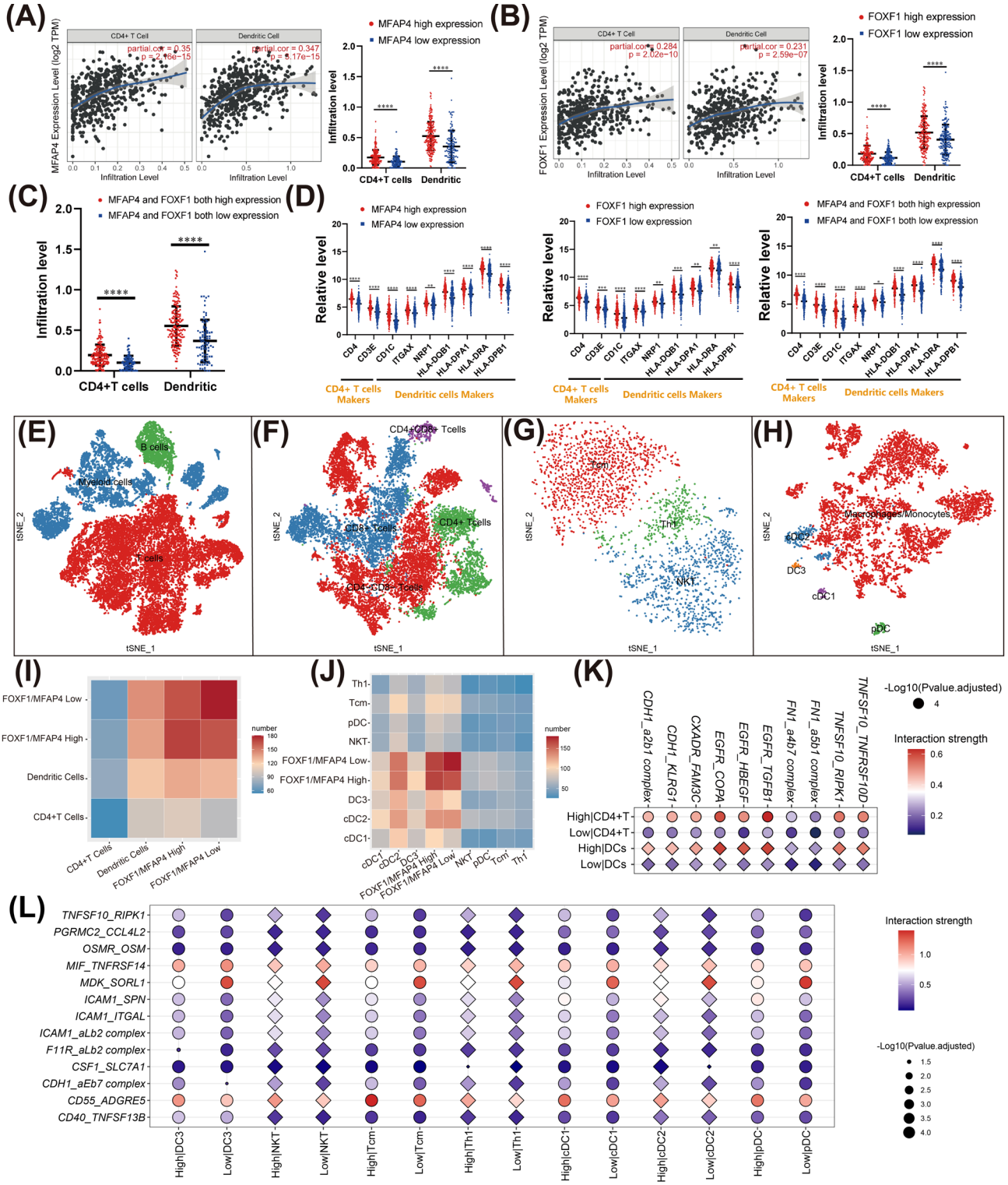

in-depth analysis using scRNA-Seq data. Figure 7e and f display the clustering and annotation of immune cells and T cells, respectively. Similarly, the subpopulations of CD4+ T cells and myeloid cells are respectively shown in Fig. 7g and h. Cell communication analysis shows that the high expression of FOXF1/MFAP4 significantly increases the interaction between LUAD cells and CD4+ T cells and DCs, which is consistent with the results of data analysis from TIMER database (Fig. 7i). The similarity is that the subpopulations of CD4+ T cells (Th1 and NKT) and DCs (cDC1, DC3 and pDC) also exhibit stronger interactions with LUAD cells overexpressing FOXF1/MFAP4 (Fig. 7j). Figure 7k demonstrates the enhanced interaction of some ligands-receptors between LUAD cells and CD4+ T cells and DCs (such as EGFR-TGFB1 and CDH1-KLRG1) due to the increased levels of FOXF1/MFAP4. Similarly, the high expression of FOXF1/MFAP4 also results in enhancement of the interactions of many ligands-receptors between LUAD cells and the subpopulation of CD4+ T cells and DCs are also

◂**Fig. 7.** The expression of FOXF1 and MFAP4 in LUAD cells is linked to immune cells infiltration and cellular communication. (**a–c**) Analysis of the relationship between the expression of FOXF1 and MFAP4 and CD4+ T cells and dendritic cells (DCs) infiltration using TIMER database. (**d**) Analysis of the association between the expression of MFAP4 and FOXF1 with the marker genes of CD4+ T cells and dendritic cells. (**e**) The tSNE plot shows that immune cells are annotated as T cells, B cells and Myeloid cells. (**f**) The tSNE plot shows that T cells are annotated as CD4 + /CD8 + T cells (Double positive T cells), CD4-/CD8- T cells (Double negative T cells), CD8 + T cells (Single positive T cells), CD4+ T cells (Single positive T cells). (**g**) CD4+ T cells are divided into Tcm, Th1 and NKT. (**h**) The tSNE plot shows that Myeloid cells are annotated as Macrophages/Monocytes, cDC2, DC3, Cdc3 and pDC. (**i**) Heatmap showing the number of ligand-receptor pairs that CD4+ T cells and DCs interact with LUAD tumor cells at different expression levels of FOXF1 and MFAP4. (**j**) Heatmap showing the number of ligand-receptor pairs that CD4+ T cells subpopulation (Tcm, Th1 and NKT) and DCs subpopulation (cDC2, DC3, cDC3 and pDC) interact with LUAD tumor cells at different expression levels of FOXF1 and MFAP4. (**k**) Using bubble plots to exhibit ligand–receptor pairs between high/low FOXF1/MFAP4 expression OSCC cells and CD4+ T cells and DCs. (**l**) Bubble plots exhibiting ligand–receptor pairs between high/low FOXF1/MFAP4 expression OSCC cells and subpopulation of CD4+ T cells and DCs (Tcm, Th1, NKT, cDC2, DC3, cDC3 and pDC). The tSNE plot was generated from "Seurat" package (version 4.4.0, https://github.com/satijalab/seurat) in R. The "ggplot2" (version 3.5.0, https://github.com/tidyverse/ggplot2) package in R was used to plot the heatmap and the bubble plot.

enhanced (Fig. 7l). These results suggest that the expression of FOXF1/MFAP4 may affect the infiltration level of CD4+ T cells and DCs by affecting the interaction between LUAD cells and immune cells.

To get insight into the relevant mechanisms of FOXF1/MFAP4 affecting the infiltration of CD4+ T cells and DCs, we further analyzed the expression of important immune factors associated with the function of CD4+ T cells and DCs. The results indicate that the expression levels of many cytokines related to the anti-tumor immune function of CD4+ T cells and DCs, such as IL-2, IL-12 and TNF-β, all are increased along with the increased levels of FOXF1/MFAP4 (Fig. 8a). In addition, GSEA indicate that the pathways associated with antitumor immunity are significantly enriched with the expression of FOXF1/MFAP4, while the pathways suppressing anti-tumor immunity exhibit a downward trend (Fig. 8b). These data indicates the function of FOXF1/MFAP4 in anti-tumor immunity (Fig. 8c).

Discussion

Despite the treatment of LUAD has made great progress, 5-year survival rate of LUAD is still very low due to its high degree of recurrence and metastasis[14]. Therefore, it is essential for us to study the new pathogenesis of LUAD and explore new possible therapeutic targets. In our study, through the comprehensive use of multi-omics data analysis and in vitro experiments, we revealed the potential function role of FOXF1/MFAP4/FAK signal axis in the metastasis of LUAD. And the increased expression of FOXF1/MFAP4 may enhance the anti-tumor ability of LUAD patients.

As an important transcription factor, FOXF1 has been reported that FOXF plays an essential role in the progression of a variety of cancers, including colon cancer, prostate cancer, and lung cancer, etc. For instance, FOXF1 can promote epithelial mesenchymal transformation during colon cancer metastasis through transcriptional activation of SNAI1[5], and enhance the growth and progression of prostate cancer by regulating the expression of extracellular signal-regulated kinase 5 (ERK5)[15]. However, as a key mesenchymal transcriptional factor essential for lung development, the expression of FOXF1 is found to be negatively correlated with the malignant state of tumor cells[4], which is consistent with the observations of this study in lung cancer. In fusion positive rhabdomyosarcoma (FP-RMS) tumor cells, FOXF1 protein binds chromatin near enhancers associated with FP-RMS gene signature, and cooperates with PAX3-FOXO1 and E-box transcription factors MYOD1 and MYOG to regulate FP-RMS-specific gene expression promoting FP-RMS tumorigenesis[16].

Heterozygous point mutations and genomic deletions involving FOXF1 have been reported in newborns with a lethal lung developmental disorder[17]. There have been various reports of FOXF1 levels being deregulated in cancer, the role of FOXF1 in carcinogenesis is still controversial. The complexity of FOXF1 role in carcinogenesis might be attributed to the observations: (1) regulation of FOXF1 expression likely utilizes a combination of chromosomal looping, differential methylation of an upstream CpG island overlapping GLI transcription factor binding sites, and the function of lung-specific long non-coding RNAs (lncRNAs); (2) genomic and epigenetic complexity of the FOXF1 Locus in 16q24.1of human chromosome[18]; (3) the complex protein regulatory network formed by FOXF1 protein. Therefore, identifying target genes of FOXF1 may provide new options for the treatment of tumors.

MFAP4, produced by vascular smooth muscle cells and highly enriched in the blood vessels of the heart and lung, has been indicate to be a carrier of the tumor associated carbohydrate sialyl-Lewis x in pancreatic adenocarcinoma[19]. Loss of MFAP4 alters the balance between myeloid and lymphoid lineages during both primitive and definitive haematopoiesis, which could significantly impact the downstream function of the immune system[20]. Emerging data suggest that MFAP4 is actively involved in the pathogenesis of remodeling-associated diseases, including fibrosis, cardiovascular disorders, aging, asthma and cancer through activation of integrin-mediated signaling as well as by modulating TGF-β pathway[21]. Human MFAP4 promoter is a TATA-less promoter that can be up-regulated by retinol and coenzyme Q10 (coQ10) in Detroit 551 cells[22]. While the function of MFAP4 in LUAD is still lacking. We here verify the important function of MFAP4 in LUAD cells migration and proliferation, and identify it as an important target gene of FOXF1 to inhibit the metastasis of LUAD cells.

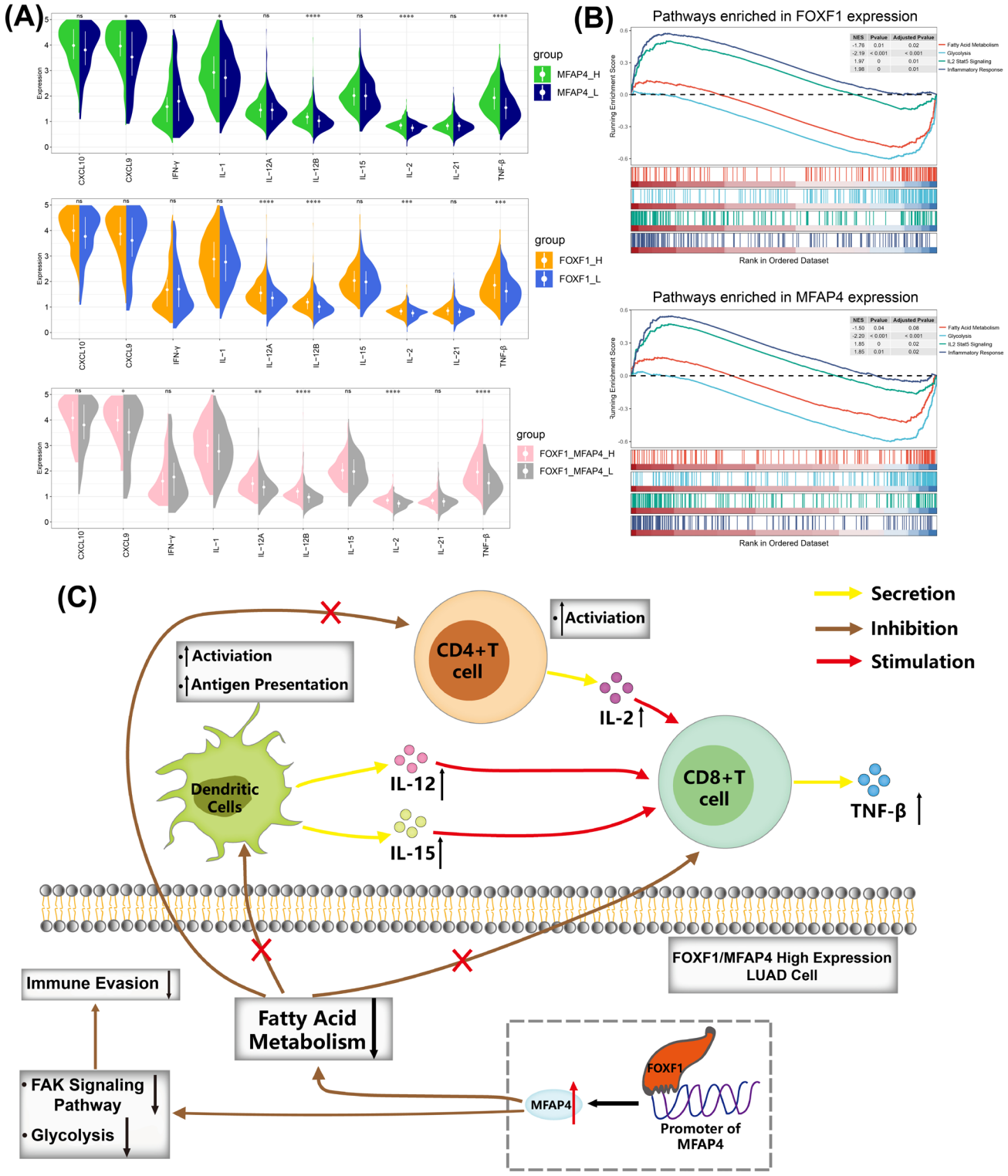

Fig. 8. Analysis of the potential mechanism of FOXF1 and MFAP4 in anti-tumor immunity of LUAD. (**a**) Expression level of immune factors associated with CD4+ T cells and DCs in FOXF1/MFAP4 high expression and low expression LUAD samples from TCGA database. (**b**) Enrichment analysis of immune-related pathways in FOXF1/MFAP4 high expression and low expression LUAD samples from TCGA database by using GSEA. (**c**) The possible mechanism of FOXF1/MFAP4 on anti-tumor immunity in LUAD. The violin vlot and the GSEA plot were generated from "ggplot2" (version 3.5.0, https://github.com/tidyverse/ggplot2) package in R.

As the critical molecule of FAK signal pathway, FAK is a non-receptor tyrosine kinase with key roles in regulating cell adhesion migration, proliferation and survival[23]. As a major driver of invasion and metastasis, the increased expression of FAK is associated with poor prognosis of cancer patient. Two main regulatory mechanisms that known to contribute to FAK activation are the interactions with membrane lipids and stretching forces applied to FAK[24]. Our study indicates that overexpression of FOXF1/MFAP4 could inhibit the phosphorylation of FAK, which may suggest that the inhibition of FOXF1/MFAP4 on the metastasis of LUAD cells is involved in inhibiting the activation of FAK signal pathway, and how these molecules inhibit the phosphorylation of FAK remains to be further studied. And our results provide a new research direction for the further study of the mechanism of metastasis of LUAD.

We here demonstrate the potential function of FOXF1 and MFAP4 in anti-tumor immunity. The content and proportion of immune cells in tumor immune microenvironment play an essential role in the growth and migration of tumor cells[25]. CD4+ T cells can target tumor cells in a variety of ways, such as eliminating them by direct lysis or indirectly regulating components in the tumor microenvironment, and affect the intensity of B cells in the process of anti-tumor immunity[26]. And also, DCs are the key antigen presenting cells that trigger T cell-mediated anti-tumor immunity[27]. High infiltration level of CD4+ T cells and DCs has been found to be significantly associated with the expression of FOXF1 and MFAP4 and some important immune factors that play key roles in anti-tumor immunity have been found to be positively related to the expression of the two genes, such as IL-12, IL-15 and IL-2. CD8+ T cells are one of the main effector cells of anti-tumor immunity, but they are usually in the functional state of T cell exhaustion when they infiltrate around tumor cells[28]. Previous studies have found that IL-12 and IL-15 secreted by DCs and IL-2 secreted by CD4+ T cells can enhance the function of exhausted CD8+ T cells and further enhance the function of anti-tumor immunity[29]. Interestingly, our study found that in the LUAD samples with high expression of FOXF1 and MFAP4, the expression level of IL-12, IL-15 and IL-2 was higher than that of low expression group. And cell communication analysis indicates that with the increase of FOXF1/MFAP4 expression, the interactions of some ligands-receptors between LUAD cells and CD4+ T cells and DCs is also enhanced. Among these interacting ligands and receptors, the reduction of CDH1 expression in intestinal epithelial cells is found to promote the recruitment of KLRG1 + GATA3 + regulatory T cells (Tregs)[30], which can inhibit the ability of immunity to clear tumor cells. Unfortunately, no study has been reported about the effect of increased expression of CDH1 in tumor cells on the level of Tregs infiltration. In this study, we for the first time observed that high expression of FOXF1/MFAP4 can enhance the interaction of CDH1-KLRG1 between LUAD and CD4+ T cells. Therefore, we speculate that the high expression of FOXF1/MFAP4 may inhibit the infiltration of Tregs by enhancing the CDH1-KLRG1 interactions between LUAD cells and Tregs. Due to the facts that the scRNA-Seq datasets in this study are not annotated to Tregs, we are unable to elucidate the detailed interactions between LUAD cells and Tregs through CDH1-KLRG1 in this study, which needs to be further studied. In addition, Natural Killer T cells (NKT) is also found to be able to enhance association with FOXF1/MFAP4-high-expressing LUAD cells through multiple ligands-receptors, such as CD55_ADGRE5, ICAM1_ITGAL and ICAM1_SPN. However, there are still few studies on the above-mentioned ligand-receptor pairs between LUAD cells and NKT, and further study is needed in the future.

In present study, GSEA shows that immune response-related pathways (IL2-Stat5-Signaling, Inflammatory-Response) are significantly up-regulated in LUAD samples with high expression of FOXF1/MFAP4, while Fatty-Acid-Metabolism and Glycolysis are down-regulated. Enhanced glycolysis in lung cancer cells inhibits T cells infiltration and activation in the tumor microenvironment, while inhibition of glycolysis enhances T cells-mediated antitumor immunity in vitro and in vivo[31]. At the same time, fatty acid can inhibit the anti-tumor activity of T cells[32] and promote the expression of T cells immune checkpoints, thus making T cells more likely to be inhibited[33]. As our research results show, the high expression of FOXF1/MFAP4 is very likely to inhibit fatty acid metabolism and glycolysis in LUAD cells, which will be more conducive to the function of T cells to exert anti-tumor immunity. Based on the above results, we speculate that the expression of FOXF1/MFAP4 in LUAD cells can enhance the anti-tumor immune function by affecting the related signal pathways in LUAD (such as fatty acid metabolism, glycolysis and FAK signal pathway) and the interactions between LUAD cells and CD4+ T cells and DCs.

In summary, our research for the first time demonstrates the potential function of FOXF1/MFAP4/FAK signaling axis in the regulation of LUAD cells' metastasis and the modulation in anti-tumor immunity, which may provide profound insights for further study of the specific potential mechanism of LUAD and develop new treatment strategies.

Materials and methods

Collection and bioinformatics analysis of public datasets

The gene array datasets, including GSE10072 (58 LUAD samples and 49 normal samples), GSE116959 (46 LUAD samples and 11 normal samples) and GSE31210 (226 LUAD samples and 20 normal samples), were downloaded from GEO database[34]. The Bulk RNA-Sequencing (RNA-Seq) data of LUAD and corresponding para-cancerous tissues (54 normal samples and 497 LUAD samples) were downloaded from TCGA database using "TCGA-biolinks" package in R[35]. The "Count" was used for subsequent differential gene expression analysis, and the "TPM" (Transcripts Per Million) was used for absolute quantitative analysis. The single cell RNA-Sequencing (scRNA-Seq) data of LUAD (GSE131907), including 2 normal lung tissue samples, 8 LUAD samples from the primary sites and 3 LUAD samples from the metastatic sites, was downloaded from GEO database. The "limma" package[36] and "DEseq2" package were used to screen the differentially expressed genes (DEGs) of gene array data and Bulk RNA-Seq data, respectively. Gene Ontology (GO) analysis, Kyoto Encyclopedia of Genes and Genomes (KEGG) and Gene Set Enrichment Analysis (GSEA) were carried out using "clusterProfiler" package. Single sample gene set enrichment analysis (ssGSEA) was performed using "GSVA" package. The "WGCNA"

package was used to build a co-expression network. Random forest prognostic model was built by "randomForest" package. The "Seurat" package was used to perform dimensionality reduction clustering, cells annotation and other related analysis of scRNA-Seq data, and the specific analysis process refers to the previously published article[37]. The "InferCNV" package[38] was used to identify LUAD cells in scRNA-Seq samples by calculating the Copy Number Variation (CNV) of all epithelial cells. The "Harmony" package[39] was used to merge different scRNA-Seq samples and perform batch correction. The "monocle2" package[40] was used for pseudotime analysis. The "CellPhoneDB" package[41] was used for intercellular interaction analysis. Kaplan–Meier Plotter database and Gene Expression Profiling Interactive Analysis (GEPIA) database were used for survival analysis. Using Immune Estimation Resource (TIMER) database to analyze the infiltration of immune cells[42]. The "Pheatmap" and "ggplot2" packages were used to visualize analysis results.

Cell culture and LUAD clinical samples

Human LUAD cell lines namely A549 and SPC-A1, human renal epithelial cell lines namely 293 T were purchased from American Type Culture Collection (ATCC) and respectively cultured in RPMI 1640 or DMEM medium supplemented with 10% fetal bovine serum (FBS, Gibco/BRL, USA) at 37 °C with 5% CO_2. A total of 7 fresh samples of human LAUD and paired normal lung tissues were provided by Shanghai Biochip Company Ltd. All samples were collected under the informed consent of the patients. And the present study was conducted according to human subject research guidelines and received Institutional Review Board approval. All clinical samples were frozen and stored at − 80 °C immediately after collection, and then used for Quantitative Real-time PCR (qRT-PCR) and Western blot analysis.

Plasmids and transfection

The exogenous expression system of FOXF1 or MFAP4 was generated by sub-cloning PCR-amplified full-length human FOXF1 or MFAP4 cDNA into plasmid pEZ-M02 (pEZ-M02-FOXF1) or pReceiver-M98 (pReceiver-M98-MFAP4). To knock down FOXF1, one short hairpin RNA (shRNA) oligo nucleotides were cloned into the pU6-GFP-puro (FOXF1-shRNA: 5′-GTGCTTCATCAAGCTACCCAA-3′). The above plasmids and negative control (NC) were synthesized by Guangzhou FulenGen Co., Ltd. To knock down MFAP4, we designed and synthesized MFAP4 specific siRNA (MFAP4 siRNA: 5′-TGGAGAGGTTTTGCCTTCA-3′) in RiboBio Co., Ltd. Before the transfection experiment, the cells were incubated with intact culture medium without antibiotics for two hours, and then the cell transfection operation was carried out according to the instructions of the transfection reagent (Zeta Life advanced DNA/RNA Transfection Reagent).

qRT-PCR

Trizol (Invitrogen) was used to extract total RNA from cells and tissues, and cDNA was synthesized by reverse transcription using FastQuantRT kit (TianGen, Beijing, China) according to the instructions. qRT-PCR was performed by standard methods using SYBR (Kangwei, Beijing, China). Shanghai Songon Biotech designed and synthesized all primers (Table S2). The mRNA expression level was calculated by the $2^{-\Delta CT}$ or $2^{-\Delta\Delta CT}$ methods and normalized to GAPDH. All experiments were performed in triplicates.

Western blot

Prepare cell or tissue protein lysates using RIPA lysis buffer (add 1 μl PMSF per 100 μl), and quantify by BCA analysis according to the instructions. Antibodies against MFAP4 (1:1000, 17661-1-AP), β-Tubulin (1:5000, 10068-1-AP) and goat anti rabbit secondary antibodies were purchased from Proteintech Group Inc, Wuhan Sanying (Wuhan, China). Antibody against FOXF1 (1:1000, A17356) was purchased from ABclonal Company. Antibodies against FAK (1:1000, AF6397) and p-FAK-Tyr397 (1:1000, AF3398) were purchased from Affinity Biosciences Company. Western blot was performed according to previously described methods[43].

Dual-luciferase reporter gene assay

MFAP4 promoter expression plasmids (pEZX-PG02-MFAP4) was constructed using firefly luciferase reporter gene vector pEZX-PG02. GAPDH promoter expression plasmids (pEZX-PL01-GAPDH) internal reference plasmids was constructed using Rinilla luciferase reporter gene vector pEZX-PL01. The specific groups were as follows: ①FOXF1:pEZX-PG02-MFAP4 + pEZ-M02-FOXF1 + pEZX-PL01-GAPDH; ②Vector:pEZX-PG02-MFAP4 + pEZ-M02-Vector + pEZX-PL01-GAPDH. 293 T cells were inoculated into 96-well plate, and then the transfection experiment was carried out as mentioned above. The transfected 293 T cells were incubated for 48 h, and then the luciferase (firefly luciferase and Rinilla luciferase) activity was detected by dual luciferase reporter system (spectramax paradigm, USA).

Wound healing assay and Transwell

To evaluate the effect of FOXF1 and MFAP4 expression on the migration of LUAD cells, A549 and SPC-A1 cells (104/mL) were seeded in 12-well plate and cultured in RPMI 1640 medium containing 10% FBS at 37 °C with 5% CO_2. After the cells were completely healed, use a sterile pipette tip to create an artificial wound along the center of each monolayer, and wash the cells twice with PBS solution. After discarding the PBS, add FBS-free RPMI 1640 medium to continue culturing the cells, and record the healing degree of the cells at 12 h, 24 h and 36 h, respectively.

In order to detect the change of invasive ability of LUAD cells, the Transwell chamber was placed in a 12-well plate. Firstly, Matrigel (Corning Incorporated) was prepared on the upper chamber to form a hydrated basement membrane. Then the LUAD cells suspension prepared by 1640 medium without serum (104/mL) were injected

into the upper chamber and the complete medium was added into the lower chamber. After 24 h, the cells on the upper surface of the chamber were erased with a cotton swab, and then the invasive cells on the lower surface were fixed and stained with 4% paraformaldehyde and 0.1% crystal violet, respectively. Randomly select 3 areas to shoot and count the number of invasion cells.

Chromatin Immunoprecipitation (chip)

Chip was performed using a kit (Thermo Fisher Scientific, 26157) according to the manufacturer's protocol. Chromatin was prepared and immunoprecipitated using antibody against FOXF1 (Novus Biologicals, AF4798). Negative control samples were prepared using control IgG antibody (Proteintech Group Inc, Wuhan Sanying, 30000-0-AP). Immunoprecipitated chromatin was analyzed by qRT-PCR using SYBR (Kangwei, Beijing, China). The primers for the MFAP4 promoter are as follows: 5′-CACATGAGGGAGCAGAGGAC-3′(F), 5′-GGAGCC AGGTGCCTACATTT-3′(R).

Statistical analysis

All statistical analyses and graph drawing are performed with R (version 4.2.2) and Graph Pad Prism (version 8.0). The Student's t test or Mann–Whitney U-test is used to compare the difference within two groups. Log-rank test is used in all survival analysis. Pearson or Spearman rank correlation test is used for correlation analysis. In all statistical analyses, $p < 0.05$ are considered significant and denoted by *, $p < 0.01$ by **, $p < 0.001$ by ***, $p < 0.0001$ by ****.

Data availability

The datasets supporting the current findings are presented within the manuscript and/or additional supporting files. They are also available from the corresponding author upon reasonable request. No original sequencing data were generated in this study. The public datasets used in the article can be found in the following public databases: GEO database (https://www.ncbi.nlm.nih.gov/geo/, GSE10072, GSE116959, and GSE131907) and TCGA database (https://www.cancer.gov/ccg/research/genome-sequencing/tcga, LUAD RNA-seq sample).

Received: 21 May 2024; Accepted: 9 September 2024
Published online: 13 September 2024

References

1. Dubin, S. & Griffin, D. Lung cancer in non-smokers. *Mo. Med.* **117**(4), 375–379 (2020).
2. Wang, S. *et al.* Machine learning reveals diverse cell death patterns in lung adenocarcinoma prognosis and therapy. *NPJ Precis. Oncol.* **8**(1), 49 (2024).
3. Sturtzel, C. *et al.* FOXF1 mediates endothelial progenitor functions and regulates vascular sprouting. *Front. Bioeng. Biotechnol.* **6**, 76 (2018).
4. Wu, C. Y. *et al.* Highly expressed FOXF1 inhibit non-small-cell lung cancer growth via inducing tumor suppressor and G1-phase cell-cycle arrest. *Int. J. Mol. Sci.* **21**(9), 3227 (2020).
5. Wang, S. *et al.* FOXF1 induces epithelial-mesenchymal transition in colorectal cancer metastasis by transcriptionally activating SNAI1. *Neoplasia* **20**(10), 996–1007 (2018).
6. Wei, H. J. *et al.* FOXF1 mediates mesenchymal stem cell fusion-induced reprogramming of lung cancer cells. *Oncotarget* **5**(19), 9514–9529 (2014).
7. Milewski, D. *et al.* FoxF1 and FoxF2 transcription factors synergistically promote rhabdomyosarcoma carcinogenesis by repressing transcription of p21Cip1 CDK inhibitor. *Oncogene* **36**(6), 850–862 (2017).
8. Pilecki, B. *et al.* Microfibrillar-associated protein 4 modulates airway smooth muscle cell phenotype in experimental asthma. *Thorax* **70**(9), 862–872 (2015).
9. Zhao, H. *et al.* High expression levels of AGGF1 and MFAP4 predict primary platinum-based chemoresistance and are associated with adverse prognosis in patients with serous ovarian cancer. *J. Cancer* **10**(2), 397–407 (2019).
10. Feng, Y. Y. *et al.* MicroRNA-147b promotes lung adenocarcinoma cell aggressiveness through negatively regulating microfibril-associated glycoprotein 4 (MFAP4) and affects prognosis of lung adenocarcinoma patients. *Gene* **730**, 144316 (2020).
11. Pan, Z. *et al.* MFAP4 deficiency alleviates renal fibrosis through inhibition of NF-kappaB and TGF-beta/Smad signaling pathways. *FASEB J.* **34**(11), 14250–14263 (2020).
12. Martinez, J. G., Carroll, R. J., Müller, S., Sampson, J. N. & Chatterjee, N. Empirical performance of cross-validation with oracle methods in a genomics context. *Am. Stat.* **65**(4), 223–228 (2011).
13. Hu, H. *et al.* AnimalTFDB 3.0: A comprehensive resource for annotation and prediction of animal transcription factors. *Nucleic Acids Res.* **47**(D1), D33–D38 (2019).
14. Greenhalgh, J. *et al.* First-line treatment of advanced epidermal growth factor receptor (EGFR) mutation positive non-squamous non-small cell lung cancer. *Cochrane Database Syst. Rev.* **3**(3), CD010383 (2021).
15. Fulford, L. *et al.* The transcription factor FOXF1 promotes prostate cancer by stimulating the mitogen-activated protein kinase ERK5. *Sci. Signal.* **9**(427), ra48 (2016).
16. Milewski, D. *et al.* FOXF1 is required for the oncogenic properties of PAX3-FOXO1 in rhabdomyosarcoma. *Oncogene* **40**(12), 2182–2199 (2021).
17. Dharmadhikari, A. V. *et al.* Lethal lung hypoplasia and vascular defects in mice with conditional Foxf1 overexpression. *Biol. Open* **5**(11), 1595–1606 (2016).
18. Dharmadhikari, A. V., Szafranski, P., Kalinichenko, V. V. & Stankiewicz, P. Genomic and epigenetic complexity of the FOXF1 locus in 16q24.1: Implications for development and disease. *Curr. Genom.* **16**(2), 107–116 (2015).
19. Guerrero, P. E. *et al.* Microfibril associated protein 4 (MFAP4) is a carrier of the tumor associated carbohydrate sialyl-Lewis x (sLe(x)) in pancreatic adenocarcinoma. *J. Proteom.* **231**, 104004 (2021).
20. Ong, S. L. M., de Vos, I., Meroshini, M., Poobalan, Y. & Dunn, N. R. Microfibril-associated glycoprotein 4 (Mfap4) regulates haematopoiesis in zebrafish. *Sci. Rep.* **10**(1), 11801 (2020).
21. Kanaan, R., Medlej-Hashim, M., Jounblat, R., Pilecki, B. & Sorensen, G. L. Microfibrillar-associated protein 4 in health and disease. *Matrix Biol.* **111**, 1–25 (2022).
22. Lin, Y. J., Chen, A. N., Yin, X. J., Li, C. & Lin, C. C. Human microfibrillar-associated protein 4 (MFAP4) gene promoter: A TATA-less promoter that is regulated by retinol and coenzyme Q10 in human fibroblast cells. *Int. J. Mol. Sci.* **21**(21), 8392 (2020).

23. Rigiracciolo, D. C. *et al.* Focal adhesion kinase (FAK) activation by estrogens involves GPER in triple-negative breast cancer cells. *J. Exp. Clin. Cancer Res.* **38**(1), 58 (2019).
24. Tapial Martínez, P., López Navajas, P. & Lietha, D. FAK structure and regulation by membrane interactions and force in focal adhesions. *Biomolecules* **10**(2), 179 (2020).
25. Zhou, K. *et al.* Targeting tumor-associated macrophages in the tumor microenvironment. *Oncol. Lett.* **20**(5), 234 (2020).
26. Melssen, M. & Slingluff, C. J. Vaccines targeting helper T cells for cancer immunotherapy. *Curr. Opin. Immunol.* **47**, 85–92 (2017).
27. Fu, C. & Jiang, A. Dendritic cells and CD8 T cell immunity in tumor microenvironment. *Front. Immunol.* **9**, 3059 (2018).
28. He, Q. F. *et al.* CD8+ T-cell exhaustion in cancer: Mechanisms and new area for cancer immunotherapy. *Brief. Funct. Genom.* **18**(2), 99–106 (2019).
29. Hashimoto, M., Im, S. J., Araki, K. & Ahmed, R. Cytokine-mediated regulation of CD8 T-cell responses during acute and chronic viral infection. *Cold Spring Harb. Perspect. Biol.* **11**(1), a028464 (2019).
30. Meinicke, H. *et al.* Tumour-associated changes in intestinal epithelial cells cause local accumulation of KLRG1(+) GATA3(+) regulatory T cells in mice. *Immunology* **152**(1), 74–88 (2017).
31. Cascone, T. *et al.* Increased tumor glycolysis characterizes immune resistance to adoptive T cell therapy. *Cell Metab.* **27**(5), 977-987. e974 (2018).
32. Peng, D. *et al.* Epigenetic silencing of TH1-type chemokines shapes tumour immunity and immunotherapy. *Nature* **527**(7577), 249–253 (2015).
33. Ma, X. *et al.* Cholesterol induces CD8+ T cell exhaustion in the tumor microenvironment. *Cell Metab.* **30**(1), 143-156.e145 (2019).
34. Clough, E. *et al.* NCBI GEO: Archive for gene expression and epigenomics data sets: 23-year update. *Nucleic Acids Res.* **52**(D1), D138–D144 (2024).
35. Colaprico, A. *et al.* TCGAbiolinks: An R/bioconductor package for integrative analysis of TCGA data. *Nucleic Acids Res.* **44**(8), e71 (2016).
36. Lu, L., Townsend, K. A. & Daigle, B. J. Jr. GEOlimma: Differential expression analysis and feature selection using pre-existing microarray data. *BMC Bioinform.* **22**(1), 44 (2021).
37. Zhang, Y. *et al.* Single-cell RNA-seq analysis identifies unique chondrocyte subsets and reveals involvement of ferroptosis in human intervertebral disc degeneration. *Osteoarthr. Cartil.* **29**(9), 1324–1334 (2021).
38. Li, F. *et al.* Relationship between CNVs and immune cells infiltration in gastric tumor microenvironment. *Front. Genet.* **13**, 869967 (2022).
39. Korsunsky, I. *et al.* Fast, sensitive and accurate integration of single-cell data with Harmony. *Nat. Methods* **16**(12), 1289–1296 (2019).
40. Ionkina, A. A. *et al.* Transcriptome analysis of heterogeneity in mouse model of metastatic breast cancer. *Breast Cancer Res.* **23**(1), 93 (2021).
41. Efremova, M., Vento-Tormo, M., Teichmann, S. A. & Vento-Tormo, R. Cell PhoneDB: Inferring cell-cell communication from combined expression of multi-subunit ligand-receptor complexes. *Nat. Protoc.* **15**(4), 1484–1506 (2020).
42. Li, T. *et al.* TIMER2.0 for analysis of tumor-infiltrating immune cells. *Nucleic Acids Res.* **48**(W1), W509–W514 (2020).
43. Chen, X. *et al.* Synergetic and antagonistic molecular effects mediated by the feedback loop of p53 and JNK between Saikosaponin D and SP600125 on lung cancer A549 cells. *Mol. Pharm.* **15**(11), 4974–4984 (2018).

Acknowledgements

Thanks to Shanghai Biochip Company Ltd for LUAD clinical samples.

Author contributions

MY conceived and supervised the article. ZW collected and analyzed the data, carried out the experiment, wrote the manuscript, and generated the figures. MX, ZJ and ZT generated the tables. PZ and MY revised the manuscript. All authors contributed to the article and approved the submitted version.

Funding

This work is supported by grants from the National Nature Science Foundation of China (32260158 and 31160233), the Science and Technology Foundation of Jiangxi Province (20142BAB204013).

Competing interests

The authors declare no competing interests.

Ethical approval and consent to participate

The study protocol was reviewed and approved by the Ethics Review Committee of the Taizhou Hospital of Zhejiang Province. All procedures performed in studies involving human participants were performed in accordance with the ethical standards of the institutional and national research committees. The research poses no more than minimal risk to patients and includes appropriate safeguards to protect the patients' rights, safety and privacy. The informed consent requirement has been waived by Ethics Review Committee of the Taizhou Hospital of Zhejiang Province. Ethical approval and informed consent were not required for the use of the reported cell lines in the present study because A549 and SPC-A1 are established cell lines.

Additional information

Supplementary Information The online version contains supplementary material available at https://doi.org/10.1038/s41598-024-72578-7.

Correspondence and requests for materials should be addressed to M.Y.